

Design of Polar Code Lattices of Small Dimension

Obed Rhesa Ludwiniananda¹, Ning Liu², Khoirul Anwar¹, and Brian M. Kurkoski²

¹Telkom University, Bandung, Indonesia

²Japan Advanced Institute of Science and Technology, Nomi, Ishikawa, Japan

Abstract—Polar code lattices are formed from binary polar codes using Construction D. In this paper, we propose a design technique for finite-dimension polar code lattices. The dimension n and target probability of decoding error are parameters for this design. To select the rates of the Construction D component codes, rather than using the capacity as in past work, we use the explicit finite-length properties of the polar code. Under successive cancellation decoding, density evolution allows choosing code rates that satisfy the equal error probability rule. At an error-rate of 10^{-4} , a dimension $n = 128$ polar code lattice achieves a VNR of 2.5 dB, within 0.2 dB of the best-known BCH code lattice, but with significantly lower decoding complexity.

I. INTRODUCTION

An n -dimensional lattice Λ is a discrete additive subgroup of the n -dimensional Euclidean space \mathbb{R}^n . In communications applications, lattices can provide shaping gain, and are integral to certain Gaussian network coding approaches including compute-forward relaying [1] and integer-forcing MIMO [2]. Low-dimension lattices with $n \leq 24$ have been well understood for some time [3], and recently results on lattices with dimension $n \geq 1000$ have appeared [4] [5]. However, there has been relatively little study of good lattices with $24 < n < 1000$, which is relevant for low-latency communications.

Construction D builds lattices from two or more component codes, which are linear binary codes. Polar code lattices are appealing because the lattice inherits the good properties of the underlying polar codes. Liu *et al.* showed that polar code lattices are AWGN good, and can achieve the capacity of the AWGN channel [4].

Polar codes have flexibility in rate selection, which is important for good lattice design. As far as we know, the only existing design of a finite-dimension lattice is by Liu *et al.*; a dimension $n = 1024$ polar code lattice [4]. The design was guided by channel capacity, but the actual design differed noticeably from what would be predicted by capacity. In high dimension, it is reasonable to use channel capacity as design guidance, but this breaks down when considering small and medium-dimension lattices. Questions still remain about the best way to design finite dimension polar code lattices.

As a multi-level construction, Construction D lattices can be designed using the decoder error rates for the component codes, under the equal error probability rule [6]. This has also been used to design Construction D' lattices based on LDPC

codes [5]; the shortcoming is that Monte Carlo simulations are slow and time-consuming. However, for binary polar codes with successive cancellation decoding, decoder error rates can be obtained using density evolution [7].

This paper contributes a design technique for polar code lattices of finite dimension. As a Construction D lattice, the challenge is to select the rates of the component codes that give the best lattice properties. Rather than using the capacity, we use the explicit finite-length code properties in the design. For a code of block length¹ n , we define ρ as the code rate such that its decoder achieves a given target error rate, as a function of the channel noise σ^2 . This allows systematic and efficient design of polar code lattices for a target error rate. Under successive cancellation decoding, the ρ function is found efficiently using density evolution. The function ρ , based on finite-length code properties, has an S-shape which is characteristic of a channel capacity curve.

Under successive cancellation decoding, a dimension $n = 128$ and $n = 256$ polar code lattice achieves VNR of 3.25 dB and 3.0 dB respectively, at WER of 10^{-4} . Under successive cancellation list decoding, a dimension $n = 128$ polar code lattice achieves VNR of 2.5 dB. This is within 0.2 dB of the best-known $n = 128$ BCH code lattice [8], and SCL decoding complexity is significantly lower than OSD decoding.

II. CONSTRUCTION D LATTICES

A. Construction D Lattice

Construction D is a type of lattice construction [3] [9]. Construction D uses multiple nested binary codes to produce a multilevel construction [10]. Let $C_0 \subseteq C_1 \subseteq \dots \subseteq C_{a-1} \subseteq C_a = \mathbb{F}_2^n$ be nested binary linear codes with generator matrices $\tilde{\mathbf{G}}_0, \dots, \tilde{\mathbf{G}}_{a-1}, \tilde{\mathbf{G}}$, respectively. Code C_i is an (n, k_i) binary with code rate $R_i = k_i/n$, and the code nesting gives:

$$\begin{aligned} R_0 &\leq R_1 \leq \dots \leq R_a \\ k_0 &\leq k_1 \leq \dots \leq k_a \end{aligned}$$

Construction D lattice Λ consists of all vectors of the form

$$\mathbf{x} = \sum_{i=0}^{a-1} 2^i \tilde{\mathbf{G}}_i \cdot \mathbf{u}_i + 2^a \tilde{\mathbf{G}} \cdot \mathbf{z}, \quad (1)$$

where $\mathbf{z} \in \mathbb{Z}^n$ and $\mathbf{u}_i = (u_{1,i}, u_{2,i}, \dots, u_{k_i,i})^t$, $i \in 0, 1, \dots, a-1$ and $u_{j,i} \in \{0, 1\}$ are information bits; operations are over the

¹The block length of a code and the dimension of a lattice are both denoted n ; for any design the block length of code is the dimension of the lattice.

This work was supported by JSPS Kakenhi Grant Number JP 19H02137. This work is also the output of the ASEAN IVO project, PATRIOT-41R-Net, financially supported by NICT, Japan.

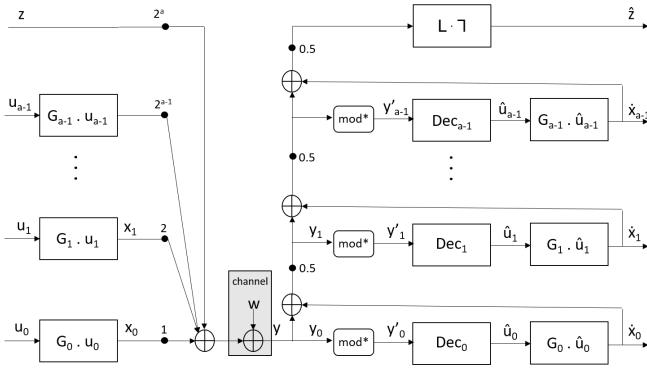


Fig. 1. Encoder, channel and multistage decoder for Construction D

real numbers and not the binary field. The full Construction D system of encoder, channel and decoder is depicted in Fig. 1.

B. Construction D Generator Matrix

The Construction D generator matrix is constructed using $\tilde{\mathbf{G}}$, a specific basis for \mathbb{F}_2^n , and k_0, k_1, \dots, k_{a-1} . The Construction D generator matrix \mathbf{G} is given by:

$$\mathbf{G} = \tilde{\mathbf{G}} \cdot \mathbf{D}^{-1}, \quad (2)$$

where \mathbf{D} is a diagonal matrix with diagonal entries d_{ii} :

$$d_{ii} = 2^{-k} \text{ for } r_{k-1} \leq i \leq r_k \quad (3)$$

with $k = 0, 1, \dots, a$.

C. VNR and Channel Model

For Construction D, the lattice volume $V(\Lambda) = |\det(\mathbf{G})|$ is

$$V(\Lambda) = 2^{an-n} \sum_{i=0}^{a-1} R_i. \quad (4)$$

The unconstrained power channel is used in this paper, where an arbitrary $\mathbf{x} \in \Lambda$ is transmitted over an AWGN channel with noise power σ^2 , and received as \mathbf{y} . This allows evaluating the coding properties of the lattice without considering a specific shaping constellation. Instead of a transmit power constraint, the lattice is constrained by the volume of the Voronoi region. The volume-to-noise ratio (VNR) is

$$\text{VNR} = \frac{V(\Lambda)^{2/n}}{2\pi e \sigma^2}. \quad (5)$$

so that VNR is the distance to the Poltyrev limit.

D. Decoding for Construction D

Construction D decoding uses successive cancellation decoding, decoding C_0 first, then C_1, C_2, \dots in order (not to be confused with successive cancellation decoding of polar codes). Before the component code decoding, a modulo operation is performed to preserve distances to $(0,1)$

$$\text{mod}^*(y_i) = |\text{mod}_2(y_i + 1) - 1| \quad (6)$$

The result of modulo operation is the input to a binary polar code decoder. The decoder produces an estimate of

the information bits \hat{u}_i and to obtain \hat{x}_i use re-encoding with generator matrix $\hat{\mathbf{x}}_i = \mathbf{G}_i \cdot \hat{u}_i$. As at the encoder side, multiplication is over the reals. This estimate \hat{x}_i is subtracted from the input, and this is divided by 2, $y_{i+1} = \frac{y_i - \hat{x}_i}{2}$. The estimated lattice point is $\hat{\mathbf{x}} = \hat{x}_1 + 2\hat{x}_2 + \dots + 2^{a-1}\hat{x}_{a-1} + 2^a\hat{z}$.

III. POLAR CODE LATTICES

A. Polar Codes and Density Evolution

Polar codes were introduced by Arıkan [11]. They provably achieve the symmetric capacity of binary input discrete memoryless channels with a low complexity decoder. Polar codes of block length n have two types of bits, k information bits $\mathcal{I} \subset \{1, 2, \dots, n\}$ and $n - k$ frozen bits; the rate is $R = k/n$. Successive cancellation (SC) decoding makes an estimate for bit position u_j using hard decisions or frozen bits \hat{u}_1^{j-1} and the recursive LLR computation:

$$L_n^{(2j-1)}(y_1^n, \hat{u}_1^{2j-2}) = 2 \tanh^{-1} \left(\tanh\left(\frac{\alpha_{n,j}}{2}\right) \cdot \tanh\left(\frac{\beta_{n,j}}{2}\right) \right)$$

$$L_n^{(2j)}(y_1^n, \hat{u}_1^{2j-1}) = (-1)^{\hat{u}_1^{2j-1}} \alpha_{n,j} + \beta_{n,j}$$

where

$$\alpha_{n,j} = L_{n/2}^{(j)}(y_1^{n/2}, \hat{u}_{1,\text{even}}^{2j-2} + \hat{u}_{1,\text{odd}}^{2j-2}),$$

$$\beta_{n,j} = L_{n/2}^{(j)}(y_1^{n/2}, \hat{u}_{1,\text{even}}^{2j-2}).$$

Polar code design assigns the position of information bits and frozen bits to indices. Mori and Tanaka described how to design polar codes using density evolution [7], under SC decoding. Under the assumption of a symmetric channel, analysis of the all-zeros codeword is sufficient. Let the probability density function of the memoryless channel LLR message be $a_1^{(1)}(x)$. Then the densities may be calculated as:

$$a_{2n}^{(2j)}(x) = (a_n^{(j)} \star a_n^{(j)})(x)$$

$$a_{2n}^{(2j-1)}(x) = (a_n^{(j)} \boxtimes a_n^{(j)})(x),$$

for $j = 1, 2, \dots, n$ where \star is standard convolution for the variable node and \boxtimes is specific check node convolution operation [12, p. 181]. For a block length n polar code, the distribution $a_n^{(j)}(x) = \Pr(L_j = x | \hat{u}_1^{j-1} = 0)$ is used to make a hard decision in position j . The probability of error in position j given positions 1 to $j-1$ are correct is:

$$p_j = \int_{-\infty}^0 a_n^{(j)}(x) dx. \quad (7)$$

The information bits \mathcal{I} are selected to be the k positions with the k smallest values of p_j .

B. Polar Code Lattices

Polar code lattices are formed using $a \geq 2$ polar codes C_0, \dots, C_{a-1} [4]. The polar code generator matrices satisfy the requirement for Construction D if the polar codes satisfy the nesting condition, $C_0 \subseteq C_1 \subseteq \dots \subseteq C_a$. For each polar code C_i the information set is \mathcal{I}_i . Then, a sequence of polar codes can be used to form a polar code lattice if $\mathcal{I}_0 \subseteq \mathcal{I}_1 \subseteq$

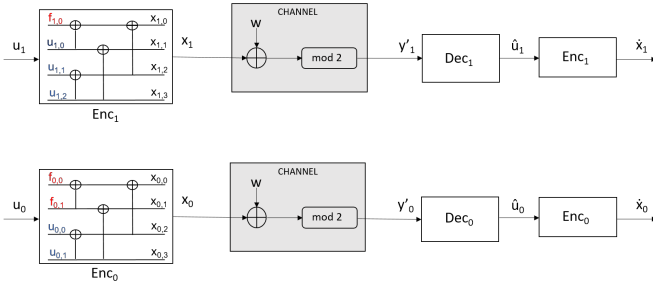


Fig. 2. Equivalent encoder, channel and decoder for multilevel decoding of Construction D assuming each level is decoded successfully.

$\dots \subseteq \mathcal{I}_a$. Thus, the information set structure can naturally form the subcodes needed for Construction D.

Example 1: Consider a basis for \mathbb{F}_2^4 given by $\tilde{\mathbf{G}}$, and nested binary codes with $k_0 = 2$, $k_1 = 3$, with generator matrices $\tilde{\mathbf{G}}_0$ and $\tilde{\mathbf{G}}_1$, given as:

$$\begin{aligned} \tilde{\mathbf{G}} &= (\mathbf{G}_m)^t \\ \tilde{\mathbf{G}} &= \begin{bmatrix} 1 & 1 & 1 & 1 \\ 0 & 1 & 0 & 1 \\ 0 & 0 & 1 & 1 \\ 0 & 0 & 0 & 1 \end{bmatrix} \end{aligned} \quad (8)$$

$$\tilde{\mathbf{G}}_0 = \begin{bmatrix} 1 & 1 \\ 0 & 1 \\ 1 & 1 \\ 0 & 1 \end{bmatrix} \quad \text{and} \quad \tilde{\mathbf{G}}_1 = \begin{bmatrix} 1 & 1 & 1 \\ 1 & 0 & 1 \\ 0 & 1 & 1 \\ 0 & 0 & 1 \end{bmatrix}.$$

From Construction D definition with $a = 2$, a lattice point satisfies

$$x = \tilde{\mathbf{G}}_0 \cdot \mathbf{u}_0 + 2\tilde{\mathbf{G}}_1 \cdot \mathbf{u}_1 + 4\tilde{\mathbf{G}} \cdot \mathbf{z}, \quad (9)$$

where $\mathbf{u}_0 = [u_{0,0}, u_{0,1}]^t$ and $\mathbf{u}_1 = [u_{1,0}, u_{1,1}, u_{1,2}]^t$ are binary vectors and $\mathbf{z} \in \mathbb{Z}^4$.

C. Equal Error Probability Rule Design Method

Due to the multilevel structure of the decoder, level i is decoded successfully only if level $i - 1$ was decoding successfully. Assuming successful decoding at all levels, each level can be seen as coding over independent channels; Fig. 2 shows Enc_0 and Enc_1 as an illustration of Example 1. Each channel is a modulo AWGN channel called AMGN (additive modulo Gaussian noise) channel. The channel noise variances are $\sigma^2, \sigma^2/4, \sigma^2/16 \dots$ for level $i = 0, 1, 2, \dots$, respectively.

A lattice decoder error is the event that $\hat{\mathbf{x}} \neq \mathbf{x}$, and P_e is the probability of this event (also, word error rate (WER) is P_e). Let $P_e(C_i, \sigma^2)$ be the probability of decoder error for C_i when used on the AMGN with noise variance σ^2 . Then by the union bound:

$$P_e \leq P_e(C_0, \sigma^2) + P_e(C_1, \frac{\sigma^2}{4}) + \dots + P_e(C_a, \frac{\sigma^2}{4^a}). \quad (10)$$

The equal error probability rule was given by Wachsmann et al. for the design of multilevel codes [6], and Construction D lattices are a special case of a multilevel code. Under the equal error probability rule, the codes C_i are selected such that $P_e(C_i, \frac{\sigma^2}{4^i})$ are equal.

Using $n = 1024$ and $a = 2$, Liu et al. gave a polar code lattice design with $(R_0, P_e(C_0)) = (0.23, \frac{1}{3} \cdot 10^{-5})$, $(R_1, P_e(C_1)) = (0.9, \frac{1}{3} \cdot 10^{-5})$, and $(R_2, P_e(C_2)) = (1, \frac{1}{3} \cdot 10^{-5})$. This design achieved VNR of 2.34 dB for $P_e = 10^{-5}$ (and VNR ≈ 2.05 dB for $P_e = 10^{-4}$) [4]. These code rates differ noticeably from those predicted by a capacity-oriented design, due to capacity losses at finite length.

IV. PROPOSED DESIGN METHOD

In this section we describe the proposed polar code lattice design, which explicitly uses the finite-length properties of polar codes with the equal error probability rule.

A. ρ Function for Binary Polar Codes

Consider a binary polar code C on the σ^2 AMGN channel and a target decoder error rate of P_{trgt} . As the code rate increases, the $\text{SNR} = 1/\sigma^2$ needed to achieve a given word-error rate also increases. Equivalently as k increases, the value of σ^2 needed to achieve P_e will decrease.

This tradeoff is expressed by a function ρ . Given σ^2 , let $\rho(\sigma^2, P_{\text{trgt}})$ be the greatest code rate such that the decoder word-error rate $P_e(C, \sigma^2)$ is not greater than a target error rate P_{trgt} . When n is small, $P_e(C, \sigma^2)$ may be noticeably less than P_{trgt} because k is an integer. Evidently, the function ρ depends on the decoding algorithm, the number of CRC bits, and the method to select the frozen bits.

For polar codes with successive cancellation decoding, ρ may be found by density evolution. Since the AMGN channel is symmetric, density evolution assuming the all-zeros code-word is sufficient. Recall that p_j is the error rate for bit position j assuming that positions 1 to $j - 1$ are correct, see (7) and \mathcal{I} is the set of information bit positions. Then the probability of word error under density evolution for polar code C is:

$$P_e(C, \sigma^2) = 1 - \prod_{j \in \mathcal{I}} (1 - p_j).$$

For a fixed channel, ρ is equal to the rate R such that the decoder error rate $P_e(C, \sigma^2)$ under density evolution is as high as possible while satisfying $P_e(C, \sigma^2) \leq P_{\text{trgt}}$.

For other decoders for which density evolution is not feasible, such as successive cancellation list decoding, ρ may be found by Monte Carlo simulations. For a given number of information bits k find the noise variances σ^2 which produce decoder error rates both above and below P_{trgt} . Interpolation may help in improving the estimate of σ^2 which will result in P_{trgt} .

The function ρ is shown in Fig. 3. For successive cancellation decoding, $n = 128, \dots, 2048$ are shown for a target error rate of $P_{\text{trgt}} = \frac{1}{3} \cdot 10^{-4}$. For SCL decoding with list size 8 and 10 CRC bits, $n = 128$ is shown for $P_{\text{trgt}} = 10^{-4}$. As expected, SC decoding requires lower rates (smaller k) to achieve the

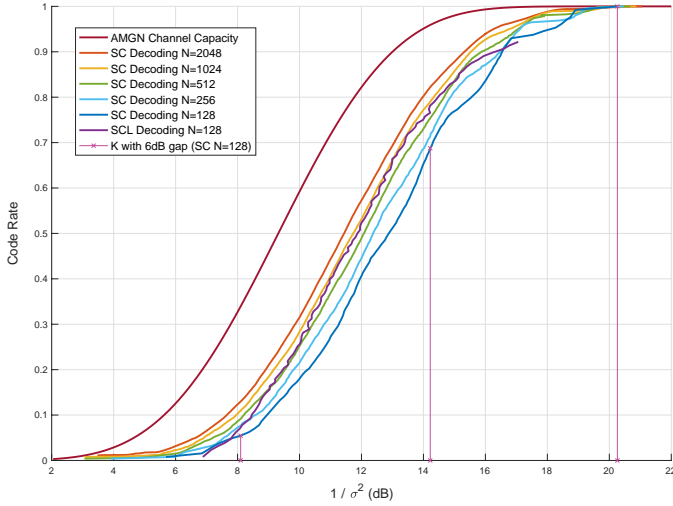


Fig. 3. The function $\rho(\sigma^2, P_{\text{trgt}})$ is the rate R for a polar code to achieve SCL decoder $P_{\text{trgt}} = 10^{-4}$ and SC decoder $P_{\text{trgt}} = \frac{1}{3}10^{-4}$ on a AMGN channel with noise σ^2 . The SCL decoder uses 10 CRC bits and decoder list size 8.

target P_e . Also shown is the capacity of the AMGN channel [4, Fig. 6] [6, Fig. 7]. Interestingly, the ρ curve exhibits the same S-shape characteristic of the capacity curve.

B. Design of Polar Code Lattices

To design a polar code lattice of dimension n , the goal is to choose k_0, \dots, k_{a-1} , or equivalently rates R_0, \dots, R_{a-1} such that the polar code lattice has the lowest possible VNR for a target probability of word error P_e . Under the equal-error probability rule, each component code C_0, C_1, \dots, C_a should have equal error rates P_{trgt} when decoding on its respective equivalent channel. Each layer sees an AMGN channel as described in Section III. Let $\sigma_0^2, \sigma_1^2, \dots$ be the AMGN noise variance for level $i = 0, 1, \dots$.

The ρ function for a polar code of block length n is used to design a polar code lattice of dimension n with a designed lattice error rate of P_e . Following the union bound (10), choose $P_e = (a + 1)P_{\text{trgt}}$ for an a -level lattice. Under the equal error probability rule, we allow $P_e(C_i, 4^{-i}\sigma^2) \approx P_{\text{trgt}}$, for $i = 0, 1, \dots, a$.

Let $\sigma_a^2 = 4^{-a}\sigma^2$ be the noise variance for which the decoder at level a achieves P_{trgt} . Since this is the uncoded level, $k_a = n$:

$$\sigma_a^2 = \rho^{-1}(n, P_{\text{trgt}}) \quad (11)$$

The probability of error in level a can be computed explicitly [5, eqn. (5)], and the inverse of this function gives:

$$\sigma_a^2 = \frac{1}{8 \cdot (\text{erfc}^{-1}(1 - \sqrt{1 - P_{\text{trgt}}}))^2}, \quad (12)$$

where erfc^{-1} is the inverse of the complementary error function.

TABLE I

POLAR CODE LATTICE DESIGNS UNDER SC DECODING AND $P_e = 10^{-4}$.

	$n = 64$	$n = 128$	$n = 256$	$n = 512$	$n = 1024$
k_0	1	7	24	68	178
k_1	40	88	192	410	866
k_2	64	128	256	512	1024
$\frac{1}{\sigma_a^2}$	20.03 dB	20.26 dB	20.47 dB	20.68 dB	20.87 dB

Once σ_a^2 is fixed, use the function ρ to find R_i for $i = 0, \dots, a - 1$:

$$R_i = \rho(4^{a-i}\sigma_a^2, P_e). \quad (13)$$

This results in nested binary codes C_0, \dots, C_{a-1} that forms a polar code lattice.

V. DESIGN EXAMPLES

In this section, we use the proposed design method and give examples of polar code lattices with $a = 2$, evaluate their error rate and complexity.

A. Polar Code Lattices Under SC Decoding

Under SC decoding, design a polar code lattice with $a = 2$, $n = 128$ and a target error rate $P_e = 10^{-4}$. Since $a = 2$, using $P_{\text{trgt}} = \frac{1}{3}10^{-4}$ and (12) to find $\sigma_2^2 = 0.0094258$, which is 20.26 dB. Let σ_1^2 be the noise seen in the equivalent AMGN channel in level i , as shown in Fig. 2. Continuing the design procedure, we seek k_1 for which σ_1^2 has a 6 dB gap from σ_2^2 , and similarly we seek k_0 for which σ_0^2 has a 6 dB gap from σ_1^2 (6 dB gap corresponds to the factor of 4). Since $\sigma_2^2 = 20.26$ dB, from Fig. 3, we obtain the design of $k_0 = 7$ at 8.26 dB and $k_1 = 88$ at 14.26 dB.

Table I shows polar code lattice designs for various dimensions n , based on density evolution result in Fig. 3. The target error rate is $P_e = 10^{-4}$.

B. Polar Code Lattices Under SCL Decoding

Successive cancellation list (SCL) decoders are considered. SCL decoding has good performance-complexity trade-off, but CRC bits are needed. In the short block-length regime, selecting the number of CRC bits is particularly important to the performance of the SCL decoder; the number of CRC bits are chosen to balance the tradeoff between reliability and code rate [13].

We use the polarization weight method [14] to allocate frozen bits, this is a channel-independent approximation method [15]. For this method, the information bits satisfy $\mathcal{I}_0 \subseteq \mathcal{I}_1 \subseteq \dots \subseteq \mathcal{I}_a$, thus the subcode condition needed by Construction D is met.

The design to obtain k_0 and k_1 is similar to the SC design. Density evolution is not suitable for SCL decoding due to list decoding. For this design we target $P_e = 3 \cdot 10^{-4}$, so $P_{\text{trgt}} = 10^{-4}$ and σ_2^2 corresponds to 19.98 dB. From Fig 3, we obtain the designs of $k_0 = 7$ at 7.85 dB and $k_1 = 95$ at 13.82 dB.

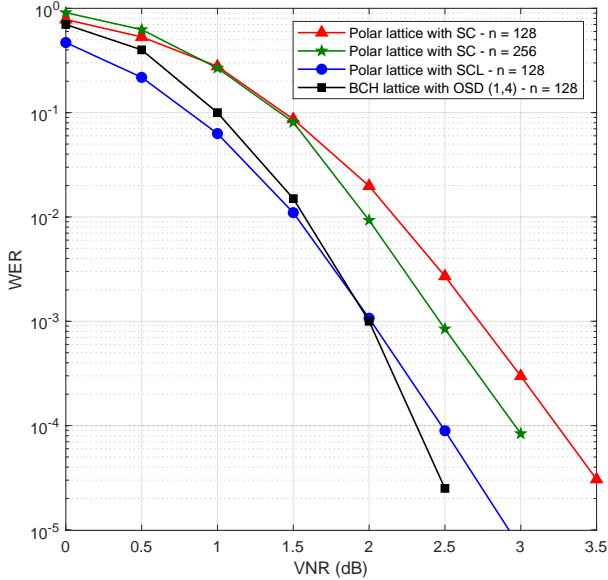


Fig. 4. WER on the unconstrained power channel, comparison between $n = 128$ BCH code code lattice with OSD decoding [8] and $n = 128, 256$ polar code lattices with SC decoding and SCL decoding (SCL with CRC-6 and list size 128).

C. Evaluation by Simulation

We evaluated these polar code lattices with their respective decoders by simulation, WER is shown in Fig. 4. For SC decoding, the $n = 128$ polar code lattice achieves a VNR of 3.25 dB. The $n = 256$ polar code lattice achieves a VNR of 3.0 dB under similar conditions. For SCL decoding, the polar code lattice achieves a VNR of 2.5 dB with 6 CRC bits and list size $L = 128$. For reference, the WER of the (128, 120), (128, 78) BCH code lattice with order-(1,4) OSD decoding achieves a VNR of 2.3 dB [8], all at a WER or $P_e = 10^{-4}$.

D. Performance-Complexity Trade-off

While polar code lattices comes within 0.2 dB of the BCH code lattice, OSD decoding [16] of BCH lattices has significantly higher complexity. SCL decoding with list size L complexity scales as $O(Ln \log n)$ while order- l OSD decoding complexity is proportional to $\sum_{i=0}^l \binom{k}{i}$.

However, for fixed n , we compare complexity by evaluating the wall clock time, the complexity as measured by the average running time to decode one codeword. Fig. 5 shows the wall clock time versus VNR to achieve WER of 10^{-4} . We found the wall clock time of OSD decoding with order (1,3) and (1,4); the wall clock time of SCL decoding is evaluated with list sizes 4, 8, 16, 32, and 128. The result shows OSD has higher wall clock time than SCL. OSD with order (1,3) requires 1.763 seconds/codeword and order (1,4) requires 140.738 seconds/codeword. The wall clock time for SCL with list size $L = 4$ with 0.023 seconds/codeword and the wall clock time with list size $L = 128$ in 0.519 seconds/codeword. The SCL decoding with $L = 128$ is better than OSD order (1,3) in both

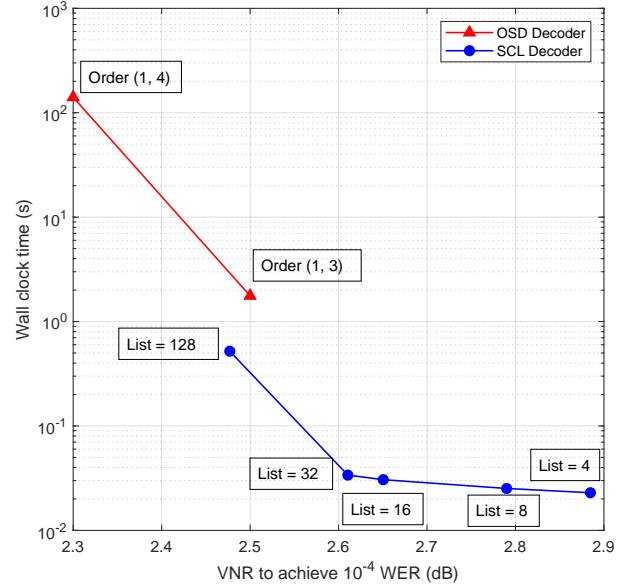


Fig. 5. Performance (VNR to achieve $P_e = 10^{-4}$) vs complexity (wall clock time) for OSD decoding and SCL decoding.

wall clock time and VNR, and it has lower wall clock time than OSD order (1,4), although the performance is worse for 0.177 dB gap.

VI. CONCLUSION

Polar code lattices can be designed in small dimension regime, using the equal error probability rule applied to a function ρ , which expresses the greatest rate which achieves a target P_e . To find the function ρ , density evolution is more efficient than Monte Carlo simulations.

While capacity-based design [4] can be used to design large-dimensional polar code lattices, this technique is not sufficient for small dimensions. As can be seen from Fig. 3, there is a significant gap between capacity and finite-length rates.

The equal-error probability rule has already been used to design Construction D' lattices based on LDPC codes [5]; the challenge is that Monte Carlo simulations are slow and time-consuming. For polar codes with successive cancellation decoding, density evolution allows obtaining probability of error quickly and efficiently.

REFERENCES

- [1] B. Nazer and M. Gastpar, "Compute-and-forward: Harnessing interference through structured codes," *IEEE Trans. on Inf. Theory*, vol. 57, no. 10, pp. 6463–6486, Oct. 2011.
- [2] J. Zhan, B. Nazer, U. Erez, and M. Gastpar, "Integer-forcing linear receivers," *IEEE Trans. on Inf. Theo.*, vol. 60, pp. 7661–7685, 2014.
- [3] J. H. Conway and N. J. A. Sloane, *Sphere packings, lattices and groups*. Springer Science & Business Media, 2013, vol. 290.
- [4] L. Liu, Y. Yan, C. Ling, and X. Wu, "Construction of capacity-achieving lattice codes: Polar lattices," *IEEE Transactions on Communications*, vol. 67, no. 2, pp. 915–928, 2019.

- [5] P. R. Branco da Silva and D. Silva, "Multilevel LDPC lattices with efficient encoding and decoding and a generalization of construction D," *IEEE Transactions on Information Theory*, vol. 65, no. 5, pp. 3246–3260, 2019.
- [6] U. Wachsmann, R. F. Fischer, and J. B. Huber, "Multilevel codes: theoretical concepts and practical design rules," *IEEE Transactions on Information Theory*, vol. 45, no. 5, pp. 1361–1391, July 1999.
- [7] R. Mori and T. Tanaka, "Performance of polar codes with the construction using density evolution," *IEEE Communications Letters*, vol. 13, no. 7, pp. 519–521, 2009.
- [8] T. Matsumine, B. M. Kurkoski, and H. Ochiari, "Construction D lattice decoding and its application to BCH code lattices," in *2018 IEEE Global Communications Conference (GLOBECOM)*, 2018, pp. 1–6.
- [9] E. S. Barnes and N. J. A. Sloane, "New lattice packings of spheres," *Canadian Journal of Mathematics*, vol. XXXV, no. 1, pp. 117–130, 1983.
- [10] H. Imai and S. Hirakawa, "A new multilevel coding method using error-correcting codes," *IEEE Transactions on Information Theory*, vol. 23, no. 3, pp. 371–377, May 1977.
- [11] E. Arikan, "Channel polarization: A method for constructing capacity-achieving codes for symmetric binary-input memoryless channels," *IEEE Transactions on Information Theory*, vol. 55, no. 7, pp. 3051–3073, 2009.
- [12] T. J. Richardson and R. Urbanke, *Modern Coding Theory*. New York, NY, USA: Cambridge University Press, 2008.
- [13] T. Murata and H. Ochiari, "On design of CRC codes for polar codes with successive cancellation list decoding," in *International Symposium on Information Theory*. Aachen, Germany: IEEE, June 2017, pp. 1868–1872.
- [14] Y. Zhou, R. Li, H. Zhang, H. Luo, and J. Wang, "Polarization weight family methods for polar code construction," in *2018 IEEE 87th Vehicular Technology Conference (VTC Spring)*, 2018, pp. 1–5.
- [15] O. Ludiwiniananda Handoko, K. Anwar, and B. Syihabuddin, "Investigating Bhattacharyya parameters for short and long polar codes in AWGN and Rayleigh fading channels," in *2019 International Conference Islam, Science and Technology (ICONISTECH)*, Bandung, Indonesia, July 2019.
- [16] M. P. Fossorier and S. Lin, "Soft-decision decoding of linear block codes based on ordered statistics," *IEEE Transactions on Information Theory*, vol. 41, no. 5, pp. 1379–1396, September 1995.